

Natural Gas Fugitive Emissions Rates Constrained by Global Atmospheric Methane and Ethane

Stefan Schwietzke,^{*,†,‡} W. Michael Griffin,^{†,‡} H. Scott Matthews,^{†,§} and Lori M. P. Bruhwiler^{||}

[†]Department of Engineering and Public Policy, Carnegie Mellon University, Baker Hall 129, 5000 Forbes Avenue, Pittsburgh, Pennsylvania 15213, United States

[‡]Tepper School of Business, Carnegie Mellon University, 5000 Forbes Avenue, Pittsburgh, Pennsylvania 15213, United States

[§]Department of Civil and Environmental Engineering, Carnegie Mellon University, Porter Hall 123A, 5000 Forbes Avenue, Pittsburgh, Pennsylvania 15213, United States

^{||}NOAA Earth Systems Research Laboratory, 325 Broadway GMD1, Boulder, Colorado 80305, United States

S Supporting Information

ABSTRACT: The amount of methane emissions released by the natural gas (NG) industry is a critical and uncertain value for various industry and policy decisions, such as for determining the climate implications of using NG over coal. Previous studies have estimated fugitive emissions rates (FER)—the fraction of produced NG (mainly methane and ethane) escaped to the atmosphere—between 1 and 9%. Most of these studies rely on few and outdated measurements, and some may represent only temporal/regional NG industry snapshots. This study estimates NG industry representative FER using global atmospheric methane and ethane measurements over three decades, and literature ranges of (i) tracer gas atmospheric lifetimes, (ii) non-NG source estimates, and (iii) fossil fuel fugitive gas hydrocarbon compositions. The modeling suggests an upper bound global average FER of 5% during 2006–2011, and a most likely FER of 2–4% since 2000, trending downward. These results do not account for highly uncertain natural hydrocarbon seepage, which could lower the FER. Further emissions reductions by the NG industry may be needed to ensure climate benefits over coal during the next few decades.



INTRODUCTION

The effectiveness of mitigating climate change using natural gas (NG) as a bridge to a renewable energy-dominated economy has been challenged by some,^{1,2} suggesting that methane (CH₄) emissions from NG systems could outweigh reduced CO₂ emissions compared to coal use. Other studies^{3–6} indicate that U.S. emissions inventories underestimate CH₄ emissions from the oil and gas industry. The increased tapping of shale formations and other unconventional NG sources—increasing production in North America and exploration activities worldwide using new technologies—adds urgency to the problem.

The U.S. Environmental Protection Agency recently amended air regulations for the oil and gas industry including targets for capturing NG that currently escapes to the atmosphere.⁷ Accurately determining CH₄ emissions that are representative of the NG industry is key for this and future policies, but it is also challenging due to the size and complexity of the NG industry.^{8,9} CH₄ is released to the atmosphere, intentionally (e.g., venting) and unintentionally (leaks), throughout the NG life cycle, which includes extraction, processing, transport, and distribution. The magnitude of life

cycle CH₄ emissions is sometimes reported as the NG fugitive emissions rate (FER), defined here as the percentage of dry production—mainly CH₄—that is lost throughout its life cycle.

Most literature FER estimates were generated using bottom-up approaches, that is, aggregating measurements and engineering estimates at different life cycle stages. Previous bottom-up studies by these^{10,11} and other authors^{1,8,9} showed that outdated and small sample size measurement data largely contribute to FER uncertainty. Local air sampling studies near NG production facilities complement the bottom-up studies,^{3,4} but they only represent a regional and temporal snapshot of the larger industry. High FER of 6–9% were reported recently using both approaches.^{1,4}

This work estimates global average FER with a top-down approach that uses long-term (1984–2011) global atmospheric CH₄ and ethane (C₂H₆) measurements to evaluate the representativeness of previous bottom-up results. These tracer

Received: March 11, 2014

Revised: June 9, 2014

Accepted: June 19, 2014

Published: June 19, 2014

gas species are the main hydrocarbon components of NG.¹² Unlike CH₄, C₂H₆ is not thought to have microbial sources,^{13,14} so its atmospheric abundance can be a useful constraint on FER. A third tracer—the carbon isotope $\delta^{13}\text{C}-\text{CH}_4$ —was employed, which provides a stronger constraint for FER than CH₄ alone. $\delta^{13}\text{C}-\text{CH}_4$ observations¹⁵ were used to exploit the fact that the isotopic values of observed atmospheric CH₄ are the result of the magnitudes and the distinct isotopic signatures of the various CH₄ sources. For instance, CH₄ emissions from fossil fuel (FF) sources are significantly less depleted in $\delta^{13}\text{C}-\text{CH}_4$ compared to microbial sources, such as wetlands.¹⁶ Previous top-down studies have estimated global or national FF CH₄ and C₂H₆ emissions^{5,13,17} using complex 3D models of the atmosphere based on (i) a priori knowledge of the approximate locations of different emissions, and (ii) spatially distributed atmospheric measurements. However, using observations to distinguish emissions from NG, oil, and coal is difficult due to close relative proximity of these sources.⁶ Quantifying the NG source is necessary to estimate FER. A detailed global bottom-up oil and coal CH₄ and C₂H₆ emissions inventory¹⁸ was developed for this study to isolate NG emissions from those associated with oil and coal.

MATERIALS AND METHODS

Global NG CH₄ and C₂H₆ emissions and uncertainties were estimated annually over the period 1985–2011 using a top-down mass balance as the difference between total emissions and other anthropogenic and natural sources. The mass balance model treats the global atmosphere as a single box, which conserves the global mass of the emissions sources and sinks (and resulting atmospheric mixing ratios), eliminating the need for complex global transport of emissions. Total annual emissions ranges were based on (i) CH₄ and C₂H₆ atmospheric measurement data from NOAA's¹⁹ and UC-Irvine's¹³ global observation networks (see Supporting Information (SI) section 1 for global average annual mixing ratios), respectively, (ii) literature atmospheric $\delta^{13}\text{C}-\text{CH}_4$ data,¹⁵ and (iii) literature ranges of global average atmospheric CH₄ and C₂H₆ lifetimes (both largely dependent on reaction with OH)^{20–24} summarized in the following subsection. The magnitudes of the uncertain anthropogenic and natural CH₄ and C₂H₆ sources were derived using a wide range of literature estimates (SI section 2) and the above-mentioned oil and coal inventory.¹⁸ Given the resulting annual NG CH₄ and C₂H₆ top-down estimates, FER was estimated using global NG production statistics in combination with thousands of NG composition samples specifying NG CH₄ and C₂H₆ contents worldwide.

Interannual variability in the OH abundance and the non-FF source strength affects FER estimates in a given year. For instance, declining OH or non-FF emissions would increase FER. This study is primarily interested in the long term FER trajectory. We therefore only accounted for interannual variations in the above model parameters where the literature indicates a long-term trend (such as in CH₄ and C₂H₆ mixing ratios shown in SI section 1). Given the lack of evidence for long-term trends in the global OH abundance²⁵ and non-FF emissions^{13,17} (for details see SI sections 1 and 2, respectively), interannual variation in non-FF emissions sources was neglected.

Using a relatively simple model, a range of scenarios was explored in order to evaluate what may be learned from the atmospheric observations, including the maximum possible global average FER. Finally, mass balance FER estimates were

substantiated using the existing 3D global chemistry transport model TMS²⁶ implemented in the CarbonTracker-CH₄ (CT-CH₄) assimilation system.²⁷ This was achieved by simulating transport of emissions throughout the global atmosphere for selected FER scenarios. The resulting CH₄ mixing ratios were then compared with observations from the global networks,^{13,19} thereby adding spatial information not available using the mass balance model.

Global Mass Balance (Box-Model). The global annual mass balance for CH₄ and C₂H₆ in year t was formulated as

$$z_{\text{CH}_4,t} = z_{\text{CH}_4,t,\text{AgW}} + z_{\text{CH}_4,t,\text{nat}} + z_{\text{CH}_4,t,\text{BBM}} + z_{\text{CH}_4,t,\text{oil}} + z_{\text{CH}_4,t,\text{NG}} + z_{\text{CH}_4,t,\text{coal/ind}} \quad (1)$$

$$z_{\text{C}_2\text{H}_6,t} = z_{\text{C}_2\text{H}_6,t,\text{BBE}} + z_{\text{C}_2\text{H}_6,t,\text{BFC}} + z_{\text{C}_2\text{H}_6,t,\text{oil}} + z_{\text{C}_2\text{H}_6,t,\text{NG}} + z_{\text{C}_2\text{H}_6,t,\text{coal}} \quad (2)$$

where $z_{\text{CH}_4,t}$ and $z_{\text{C}_2\text{H}_6,t}$ are the total annual global CH₄ and C₂H₆ emissions, respectively. The CH₄ emissions sources include agriculture/waste/landfills (AgW), natural sources (nat), biomass burning methane (BBM), oil life cycle fugitive emissions (oil; CH₄ and C₂H₆), NG life cycle fugitive emissions (NG; CH₄ and C₂H₆), and coal life cycle fugitive and “other energy and industry” emissions (coal/ind). The C₂H₆ emissions sources also include biomass burning ethane (BBE; savanna and grassland fires, tropical and extratropical forest fires, agricultural residue burning), biomass fuel combustion (BFC), and coal life cycle C₂H₆ emissions (coal; see below for “other energy and industry” C₂H₆ emissions). The literature-based CH₄ and C₂H₆ emissions ranges are summarized in the Materials and Methods subsections (non-FFs and FFs) below. The system boundaries for the CH₄ sources vary slightly among studies, but are largely consistent with those described for modeling with TMS (SI Table S1). Mass balances were solved for $z_{\text{CH}_4,t,\text{NG}}$ and $z_{\text{C}_2\text{H}_6,t,\text{NG}}$ independently using the ranges for all other source categories. The annual emissions $z_{\text{CH}_4,t}$ were estimated using eq 4, which is the solution to differential eq 3, giving $z_{\text{CH}_4,t}$. The annual emissions $z_{\text{C}_2\text{H}_6,t}$ were estimated using eq 5:

$$dC_{\text{CH}_4,t}/dt = z_{\text{CH}_4,t} - 1/\tau \times C_{\text{CH}_4,t} \quad (3)$$

$$z_{\text{CH}_4,t} = (C_{\text{CH}_4,t} - C_{\text{CH}_4,t-1} \times e^{-1/\tau}) \times (\tau \times (1 - e^{-1/\tau}))^{-1} \quad (4)$$

$$z_{\text{C}_2\text{H}_6,t} = C_{\text{C}_2\text{H}_6,t} \times \text{SF}_{\text{C}_2\text{H}_6} \quad (5)$$

where $C_{\text{CH}_4,t}$ is the annually observed global average CH₄ dry air mole fraction (in ppb) in year t multiplied by the conversion factor 2.767 Tg CH₄/ppb²⁸ in order to convert mole fractions to mass units for the global atmosphere (see SI section 1 for details). For the global average atmospheric lifetime of CH₄, τ , a range of 9.1–9.7 years was chosen, which includes the mean values from four recent studies.^{20–23} The scaling factor $\text{SF}_{\text{C}_2\text{H}_6}$ converts the annually observed global average C₂H₆ dry air mole fraction $C_{\text{C}_2\text{H}_6,t}$ into the annual emissions burden $z_{\text{C}_2\text{H}_6,t}$, which is based on 3D-modeling²⁴ and has been applied recently elsewhere.¹³ Given uncertainties of up to 45% due to the reaction rate with and mixing ratios of OH,²⁴ the average and upper bound values of $\text{SF}_{\text{C}_2\text{H}_6}$ (corresponding to a higher global budget for estimating upper bound FER), 0.018 and 0.026 Tg C₂H₆/ppt, respectively, were used.

Table 1. Summary of Global Non-FF Emissions Estimates Used in 3D-Forward-Modeling (TMS) and Ranges for Box-Modeling. Units Are Tg/yr^a

box-model (const. over time ^c)	CH ₄					C ₂ H ₆		
	natural	ag/waste/landfills	BBM	soil sink ^b	total	BBE	BFC	total
low	130	130	25	−25	260	1.6	0.6	2.2
medium	182	200	43	−25	400	3.6	2.3	5.9
high	235	270	60	−25	540	5.2	4.0	9.2
3D-model (avg. 1980–2011)	215 ^d	194 ^e	16 ^f	−40	385	n/a	n/a	n/a

^aNotes: Ag – Agriculture; BBM – Biomass burning methane; BBE – Biomass burning ethane; BFC – Biomass fuel combustion. ^bBox-model data from ref 17, 3D-model data from ref 41. ^cInterannual variations during 1980–2011 were ignored due to lack of long-term trends in OH and non-FF sources, and focus on long-term FER trajectory (see also text above). ^dAnnual emissions and seasonal cycle from ref 42. ^eAnnual emissions from ref 43, seasonal cycle from ref 44. ^fAnnual emissions from refs 45 and 46, seasonal cycle from ref 47.

The global mass balance using atmospheric $\delta^{13}\text{C}-\text{CH}_4$ measurements constrains FER based on the fact that the various CH₄ sources carry distinct isotopic CH₄ signatures. The $^{13}\text{C}:^{12}\text{C}$ ratio of CH₄, δ (in ‰), can be expressed as²⁹

$$\delta = (R_{\text{sample}}/R_{\text{standard}} - 1) \times 1000 \quad (6)$$

where $R = (\text{rare isotope/abundant isotope})$. The global mass balance for three CH₄ source categories can be formulated for each year as¹⁶

$$z_{\text{CH}_4,t} = z_{\text{mic},t} + z_{\text{FF},t} + z_{\text{BBM},t} \quad (7)$$

$$\delta_{\text{qCH}_4,t} = \delta_{\text{mic}} * z_{\text{mic},t} + \delta_{\text{FF}} \times z_{\text{FF},t} + \delta_{\text{BBM}} \times z_{\text{BBM},t} \quad (8)$$

where $z_{\text{mic},t}$, $z_{\text{FF},t}$ and $z_{\text{BBM},t}$ refer to the microbial, FF, and BBM fraction of total annual CH₄ emissions, respectively, and $z_{\text{mic},t}$ includes all natural and agriculture/waste/landfills sources. The different CH₄ emissions sources are aggregated to only three emissions categories in order to avoid an under-constrained system of two linear equations (eq 7 and eq 8). The equation system is solved for $z_{\text{mic},t}$ and $z_{\text{FF},t}$ as an optimization problem (eq 10 through eq 15), and $z_{\text{BBM},t}$ is considered at least 25 Tg CH₄/yr (see literature review in SI section 2). The literature provides wide ranges of source- (and geography-) specific isotopic signatures. For instance, Finnish subarctic wetlands range between −65‰ and −69‰³⁰ compared to −51‰ and −53‰ from landfills.¹⁶ West Siberian NG associated with oil production (high CH₄ content) has been measured around −50‰,³⁰ whereas mature dry gas can range approximately −20‰.³¹ The isotopic signatures δ_{mic} , δ_{FF} , and δ_{BBM} in this model are based on weighted averages of each emissions category from 13 literature sources,¹⁶ and lie within the range of −59 to −63‰, −38 to −42‰, and −22 to −26‰, respectively. The total annual CH₄ emissions burden $z_{\text{CH}_4,t}$ is the same as in eq 4, and the flux weighted mean isotopic ratio of all CH₄ sources²⁹ is

$$\delta_{\text{q},t} = \alpha \delta_a + \varepsilon - \frac{\varepsilon(1 + \delta_a/1000)}{z_{\text{CH}_4,t}} \times \frac{dC_{\text{CH}_4,t}}{dt} + \frac{d\delta_a}{dt} \times \frac{C_{\text{CH}_4,t}}{z_{\text{CH}_4,t}} \quad (9)$$

where $\alpha = (1 + \varepsilon/1000)$ is the isotopic fractionation factor associated with photochemical CH₄ destruction, for which $\varepsilon = -6.3$ ‰.¹⁶ As described in more detail in SI section 1, the global annual means of measured δ_a range between −47.0‰ and −47.3‰ throughout 1988–2011.^{15,32,33} Given (i) the lack of pre-1988 data, (ii) the reliance on unpublished post-2006 data,³² (iii) and the low sensitivity of the above δ_a range on

FER (see SI section 3.1), this model assumes a constant δ_a of −47.1‰. Equation 7 and eq 8 were rearranged to give:

$$z_{\text{FF},t} = \frac{\delta_{\text{q},t} \times z_{\text{CH}_4,t} - \delta_{\text{mic}} \times (z_{\text{CH}_4,t} - z_{\text{BBM},t}) - \delta_{\text{BBM}} \times z_{\text{BBM},t}}{\delta_{\text{FF}} - \delta_{\text{mic}}} \quad (10)$$

$$z_{\text{mic},t} = z_{\text{CH}_4,t} - z_{\text{FF},t} - z_{\text{BBM},t} \quad (11)$$

where units for $z_{\text{CH}_4,t}$ and δ are Tg CH₄/yr and ‰, respectively. The optimization problem is to minimize eq 10, such that

$$z_{\text{BBM},t} \geq 25 \quad (12)$$

$$-59 \geq \delta_{\text{mic}} \geq -63 \quad (13)$$

$$-38 \geq \delta_{\text{FF}} \geq -42 \quad (14)$$

$$-22 \geq \delta_{\text{BBM}} \geq -26 \quad (15)$$

Equation 12 ensures that there are only two unknowns in the problem of two linear equations. CH₄ emissions from NG $z_{\text{C13CH}_4,t,\text{NG}}$ (based on isotope observations) are the difference between FF emissions from the isotope mass balance and coal/oil emissions, which are described in more detail below:

$$z_{\text{C13CH}_4,t,\text{NG}} = z_{\text{FF},t} - z_{\text{CH}_4,t,\text{coal/ind}} - z_{\text{CH}_4,t,\text{oil}} \quad (16)$$

Finally, FER is estimated using eq 17 through eq 19:

$$\text{FER}_{\text{CH}_4,t} = z_{\text{CH}_4,t,\text{NG}} / (P_{\text{dry},t} \times \text{WF}_{\text{down},\text{CH}_4,t}) \quad (17)$$

$$\text{FER}_{\text{C}_2\text{H}_6,t} = z_{\text{C}_2\text{H}_6,t,\text{NG}} / (P_{\text{dry},t} \times \text{WF}_{\text{down},\text{C}_2\text{H}_6,t}) \quad (18)$$

$$\text{FER}_{\text{C13CH}_4,t} = z_{\text{C13CH}_4,t,\text{NG}} / (P_{\text{dry},t} \times \text{WF}_{\text{down},\text{CH}_4,t}) \quad (19)$$

where $P_{\text{dry},t}$ is the global dry production of NG³⁴ converted from volume to weight units (see our bottom-up inventory¹⁸ for details), and $\text{WF}_{\text{down},\text{CH}_4,t}$ and $\text{WF}_{\text{down},\text{C}_2\text{H}_6,t}$ are the downstream NG weight fractions of CH₄ and C₂H₆, respectively.

Global 3D Model. Three-dimensional forward simulations of CH₄ emissions using the global chemistry transport model TMS²⁶ complement the box-model approach. Forward simulations in this work cover the period 1989–2011, and measurements are the same as used for the box-model. The following five different zones were distinguished in order to analyze the spatial differences ignored in the box-model: polar Northern Hemisphere (PNH, 53.1°N–90°N), temperate Northern Hemisphere (TNH, 17.5°N–53.1°N), the tropics (17.5°S–17.5°N), temperate Southern Hemisphere (TSH, 17.5°S–53.1°S), and polar Southern Hemisphere (PSH, 53.1°S–90°S). These zones are predefined in CT-CH₄,²⁷ and

Table 2. Summary of Oil and Coal/Industry CH₄ and C₂H₆ Emissions, and Downstream NG Composition in the Bottom-up Inventory.¹⁸

			units	CH ₄			C ₂ H ₆ ^a		
				1985–1999	2000–2005	2006–2011	1985–1999	2000–2005	2006–2011
Emissions									
oil	low	Tg/yr	5	6	6	4.4	5.0	5.2	
	medium		14	16	17	5.5	6.3	6.6	
	high		41	48	51	7.6	8.8	9.2	
coal/industry	low		43	44	55	0.0	0.0	0.0	
	medium		48	49	61	0.3	0.3	0.4	
	high		56	57	71	0.6	0.6	0.8	
Composition									
downstream NG ^b	low	wt %	85			7.2			
	medium		86			7.4			
	high		87			7.7			

^aRanges of oil and coal/industry C₂H₆ emissions are due to uncertainties in C₂H₆ content of fugitive hydrocarbon emissions. ^bDownstream NG composition was estimated for use with dry production statistics (shows averages over 1985–2011) to estimate life cycle FER (as described above). Results are based on a mass balance of upstream NG, downstream NG, and natural gas liquids at the processing stage (see box-model Materials and Methods). Low and high values represent 95%-C.I.

briefly discussed in SI section 3.2. Emissions were simulated for 11 individual CH₄ source/sink categories including NG, oil, coal/industry, wetlands, soils, oceans, termites, wild animals, agriculture/waste/landfills, and biomass burning methane (all as described above). Emissions were simulated for each source separately, which allows tracking the individual contributions of total CH₄ mixing ratios. Estimating source-specific contributions is key for analyzing the underlying causes of potential spatial differences between simulations and observations. These spatial differences mainly occur because the various sources emit in specific world regions, which helps to distinguish emissions sources using the measurements from the global monitoring networks.

Model Values of Nonfossil Fuel Emissions Categories Based on Literature Review. This section describes the range of non-NG CH₄ and C₂H₆ emissions values chosen as inputs in the box-model (eqs 1, 2, 10, and 11) and the 3D-model. Non-FF CH₄ emissions ranges were selected based on five of the most recent inversion studies^{27,35–38} and two literature reviews,^{39,40} which is described in more detail in the SI (section 2), and summarized in Table 1. In the box-model, most likely FER assumes total non-FF CH₄ sources of 400 Tg/yr (medium non-FF scenario), and upper bound FER is associated with non-FF CH₄ sources of 265 Tg/yr (low non-FF scenario). The corresponding medium and low scenario C₂H₆ estimates are 5.9 Tg/yr and 2.2 Tg/yr, respectively. High CH₄ and C₂H₆ scenarios were selected such that low and high values represent a normal distribution around the medium values. Three-dimensional forward simulations were carried out with TMS for eight individual non-FF CH₄ source/sink categories (totaling on average 385 Tg/yr). The global soil CH₄ sinks used in both models cover the range of literature values: 25 Tg/yr,³⁶ 30 Tg/yr,³⁵ and 38 Tg/yr.³⁸ The total non-FF emissions in the 3D simulation and in the medium box-model scenario are very similar (difference is ~3% of global CH₄ budget), which allows direct comparison of box-model results with the 3D-model (the same oil and coal estimates were used in both models).

Model Values of Fossil Fuel Emissions Categories from Bottom-up Inventory. This section briefly summarizes the methods and data used to estimate CH₄ and C₂H₆

emissions from oil and coal production, processing and transport (in eqs 1 and 2) as well as downstream NG composition (eqs 17–19) applied in the box-model and the 3D-model. This summary is based on a global bottom-up FF inventory developed by these authors.¹⁸ Here, only the general methodology and major parameters are reviewed. The inventory is based on country-level NG, oil, and coal production data,³⁴ a range of literature emissions factors (EFs, see below for literature sources), and observational gas flaring data.^{48,49} EFs describe the amount of hydrocarbon gas emitted to the atmosphere per unit of fuel produced, and EFs are the basis for comparing greenhouse gas (GHG) emissions among different fuels or technologies in life cycle assessment. The inventory also includes hydrocarbon composition data from thousands of samples including NG and oil wells, both of which produce NG and oil.¹² The hydrocarbon composition data is necessary for deriving FER from estimated total amounts of global NG CH₄ ($z_{\text{CH}_4,\text{NG}}$) and C₂H₆ ($z_{\text{C}_2\text{H}_6,\text{NG}}$) emissions.

Emissions factors (EF) related to the oil life cycle were reviewed from four studies,^{50–53} which span an order of magnitude. The EFs include fugitive emissions from oil production, processing, and shipping as well as hydrocarbon emissions from incompletely flared gas. The EF selected from these studies⁵¹ is 50% below the mean of the lowest^{52,53} and highest⁵⁰ literature EF. This selection assures that the upper bound FER from the box-model is a conservative estimate, that is, box-model FER could be lower if oil emissions were in fact higher. Emissions from marketed (i.e., not flared/vented or repressured) associated NG production at oil wells are counted toward FER. The detailed procedure for allocating emissions between oil and NG production is described in the bottom-up inventory.¹⁸ Country-specific EFs related to the coal life cycle^{50,54–56} distinguish different types of coal production. Comparison of different global coal production estimates (and Chinese coal production in particular) suggests that the total emissions estimate in the inventory may be an underestimate. Thus, analogously to the oil emissions estimates above, FER could be lower than box-model results if coal emissions were in fact higher.

Table 2 summarizes the results from the bottom-up inventory¹⁸ including oil and coal CH₄ and C₂H₆ emissions over different time periods as well as global average downstream NG hydrocarbon composition (related to dry production statistics). Medium oil CH₄ emissions increase from 14 Tg/yr (mean during 1985–1999) to 17 Tg/yr (mean during 2006–2011), and medium coal/industry CH₄ emissions increase from 48 Tg/yr to 61 Tg/yr over the same periods. Medium oil C₂H₆ emissions increase from 5.5 Tg/yr to 6.6 Tg/yr over the same periods, and coal/industry C₂H₆ emissions are relatively small given the low coal-bed gas C₂H₆ content.¹⁸ Downstream NG CH₄ and C₂H₆ contents averaged throughout 1984–2011 range from 85 to 87 wt % and 7.2–7.7 wt %, respectively, while C₂H₆ content decreased from 7.8–6.8 wt % over this period due to increased C₂H₆ extraction for NG liquids.¹⁸

Industry (public power and heat, other energy industries, transportation, residential and other sectors, industrial processes, FF fires) emissions were adopted from EDGAR v4.2.⁴³ C₂H₆ emissions estimates from this source were unavailable, and were not accounted for in the box-model. FER could in fact be lower than box-model results if industry is a significant C₂H₆ source. Three different FER scenarios (ranging from 2 to 6% FER; see SI for details) were simulated in TMS to analyze which FER is most consistent with spatially distributed observations.

Spatial Distribution of CH₄ Emissions. Spatial CH₄ emissions grid maps were developed in order to perform 3D simulations of the global atmosphere in TMS. A detailed description of the grid map development as well as the results is provided in the bottom-up inventory,¹⁸ and briefly summarized here. The spatial distribution of FF emissions *within* each country was adopted from EDGAR v4.2,⁴³ which is based on population density and other proxies. The absolute FF emissions in the grid maps were scaled based on the FF estimates summarized in the previous subsection. Due to the emissions differences between this work and EDGAR for a given country, the spatial distribution of the scaled grid maps differs from EDGAR on a global scale, but not within individual countries. In contrast to FF, other source categories have a distinct seasonal emissions cycle. EDGAR's agriculture/waste/landfills category annual emissions grid maps were decomposed into monthly grid maps, and scaled to a seasonal cycle as defined in SI Table S1. Agriculture/waste/landfills annual totals were linearly extrapolated from 2008 (last year in EDGAR) to 2011 using the last 10 years available in EDGAR. Literature spatial CH₄ emissions distribution was adapted for natural^{57,58} and BBM⁴⁷ categories.

RESULTS

Global average FER from the NG life cycle was estimated in a top-down approach to better understand industry representative CH₄ emissions. This study is based on global spatially distributed CH₄, $\delta^{13}\text{C}-\text{CH}_4$, and C₂H₆ measurements over three decades. A global box-model was developed and an existing 3D emissions transport model was used to attribute total emissions to different sources, thereby taking into account uncertainties in atmospheric lifetimes of measured species as well as non-NG source estimates.

Global box-model. The most likely global FER of 2–4% on average during 2004–2011 (Figure 1) is consistent for CH₄, $\delta^{13}\text{C}-\text{CH}_4$, and C₂H₆ observations. These estimates assume (i) mean literature emissions values for each of the other source

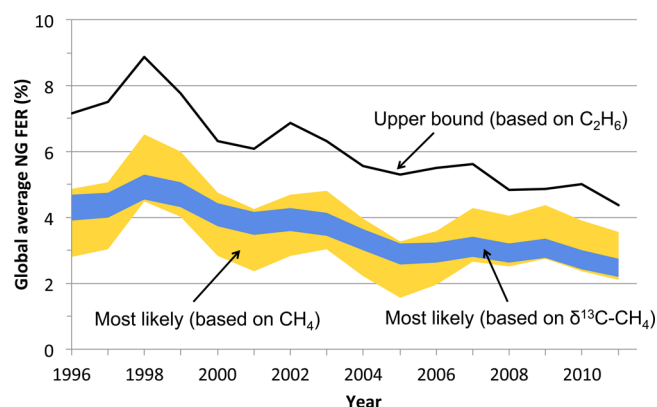


Figure 1. Summary of possible global NG fugitive emissions rates (FER) – in % of dry production – based on a global mass balance using different tracer gases. The upper bound represents a combination of assumptions from the literature including high global emissions (totaling 16.2 Tg C₂H₆/yr on average since 2000 using UC-Irvine observations¹³ and Rudolph²⁴ C₂H₆ lifetime uncertainty) and low magnitude of other C₂H₆ sources (7.4 Tg C₂H₆/yr on average since 2000). The orange and blue bands mark the range for CH₄ lifetimes between 9.1 and 9.7 years and mean literature values of other CH₄ sources (totaling 467 Tg CH₄/yr on average since 2000 including soil sink) using NOAA observations.¹⁹ FER is shown for the longest consecutive observation time series available (pre-1996 data are shown in SI Figures S5, S7).

categories listed above, and (ii) global total oil and coal CH₄ emissions from this study's emissions inventory (medium values in Table 2), which agree well (2.5% difference) with EDGAR,⁴³ that is, the commonly used a priori FF database in global top-down CH₄ modeling. The upper bound global FER averaged over the last five years of observations is 5.0% (4.4% in 2011) based on C₂H₆ observations (Figure 1). The upper bound assumes (i) a C₂H₆ lifetime corresponding to the largest global average sink in the literature, (ii) a lower bound FF C₂H₆ content (Table 2), and (iii) a lower bound BBE/BFC C₂H₆ source estimate (Table 1). Details of the budgetary implications of the upper bound FER relative to the literature are illustrated in SI Figure S8. Results indicate upper bound FER of ~6% in the early 2000s, mainly due to lower FF production compared to later years. Note that FER peaks shown for some years in Figure 1 are likely due to interannual variation in natural sources.¹³ Our upper bound throughout 1985–1999 is on average 9.3% (SI Figure S7). This temporal decline in FER is consistent with earlier work suggesting a decrease in FF C₂H₆ emissions.^{13,14} Emissions reductions per unit of production (FER) in this work imply industry efficiency improvements, although the decline would be less steep if coal and oil EFs also declined over time (increased oil and coal production over time are accounted for). Global average CH₄ and $\delta^{13}\text{C}-\text{CH}_4$ data provide weaker constraints for upper bound FER, mainly due to literature source estimate uncertainties. Assuming lower bound estimates for natural, agriculture/waste/landfills, and BBM sources *simultaneously* would lead to FER of 8% or higher averaged during 2004–2011 (SI Figure S5). Yet, Figure 1 shows that such high FER is inconsistent with the C₂H₆ data.

Natural hydrocarbon seepage may be an additional significant source of atmospheric CH₄ and C₂H₆ not currently accounted for in most top-down studies.¹⁷ Visible macro-seeps, marine seepage, microseepage, and geothermal/volcanic areas may contribute between 40 and 60 Tg CH₄/yr and 2–4 Tg C₂H₆/yr globally.⁵⁹ While not included in Figure 1, adding 40

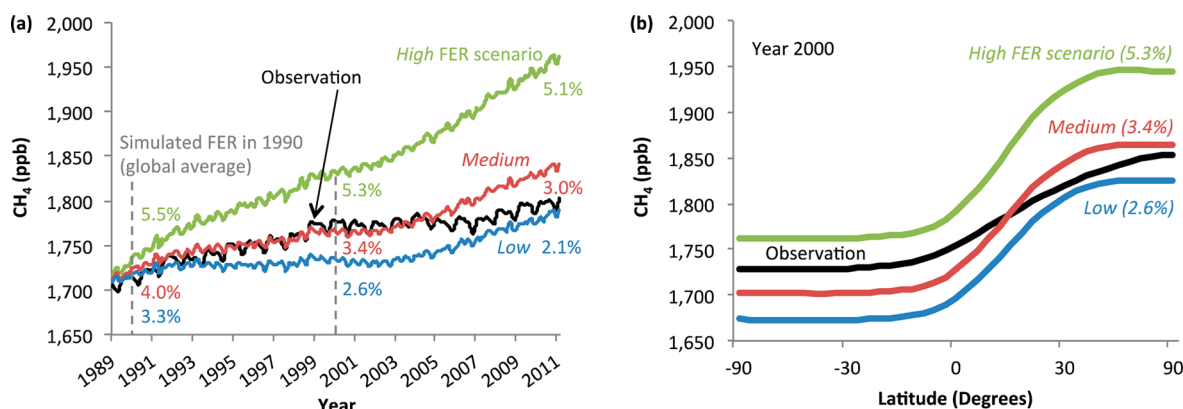


Figure 2. TM5 global average forward modeling results for three regionally and temporally distinct FER scenarios (see SI Table S4 and Figure S9) as well as NOAA's measurements.¹⁹ (a) Global average dry air mole fractions; see refs 65 and 66 for estimating global averages from spatial distributions. (b) CH₄ dry air mole fractions across 41 latitudinal bands in year 2000 (see SI Figure S10 for additional years).

Tg CH₄/yr and 2 Tg C₂H₆/yr in the model would reduce FER by about two percentage points (constant over time). The magnitude of the above seepage estimates have been challenged.¹³ Yet, having excluded any seepage in our main results (Figure 1) emphasizes that our FER may be overestimated.

The decline in global FER is 0.1 and 0.3 percentage points per year since 1985 based on most likely (CH₄ and $\delta^{13}\text{C}$ -CH₄ observations) and upper bound results (C₂H₆ observations), respectively. This assumes that the declines in measured C₂H₆ levels (or CH₄ growth rates⁶⁰) are attributed to NG emissions reductions. Kirschke et al.¹⁷ find little if any long-term natural, agriculture/waste/landfill, and BBM emissions reductions over this period. Kirschke et al.¹⁷ results, along with the findings presented here, suggest that the declines in measured mixing ratios (or growth rates thereof) can be attributed to NG emissions reductions. This is also consistent with recent top-down C₂H₆ studies^{13,14} suggesting reductions in total FF emissions where Aydin et al.¹⁴ concluded that global declines in the C₂H₆ mixing ratios were due to decreased flaring and venting of NG (see also SI Figure S8). Also, recent direct CH₄ measurements at 190 NG production sites in the U.S. by Allen et al.⁸ indicate lower overall CH₄ emissions from production (well pad) activities than previous measurement data used in EPA's 2013 GHG inventory.⁵¹ Note that increased NG, oil, and coal production over time⁶¹ was incorporated in the modeling presented here. The FER decline may be less pronounced if oil and coal emissions per unit of production also decreased since 1985. Atmospheric chemistry may also explain changes in CH₄ and C₂H₆ mixing ratios. However, Montzka et al.⁶² recently found a small interannual atmospheric OH variability of $2.3 \pm 1.5\%$ during 1998–2007, which suggests that increased sink strength is an unlikely alternative explanation for declining FER.

Global 3D-Model. Most-likely FER estimates from the mass balance are supported by the global chemistry transport model TMS²⁶ and the spatial distribution of CH₄ mixing ratios as an indicator of source strength.⁶³ Using three different FER scenarios ranging from about 2–6% FER (see SI Table S4 and Figure S9), the TMS was used to simulate spatially distributed CH₄ sources and sinks from 1989 to 2011. As shown in Figure 2a, the medium FER scenario is a reasonable fit globally throughout the 1990s (3–4% FER) compared to 3% and 5% in the box-model (SI Figure S5) for CH₄ lifetimes (τ) of 9.7 and 9.1, respectively. In the 2000s, TMS suggests a most likely FER

of ~3% dropping to just over 2% in 2010 compared to 2–4% in the box-model depending on τ . Given that τ used in TMS is approximately 9.45, most likely estimates of both models agree within one percentage point FER.

The following spatial analysis is useful for investigating whether the a priori emissions source attribution (Tables 1 and 2) is reasonable, or if, for instance—, underestimated FER scenarios were compensated by overestimated other source categories. Simulations and measurements across 41 latitudinal bands (intervals of 0.05 sine of latitude) are shown in Figure 2b as an indicator of the interhemispheric gradient (for year 2000; see SI Figure S10 for additional years). The spatial fit of simulations and measurements can be used as a proxy for the attribution of sources. About 96% of NG CH₄ emissions in the emissions grid maps simulated with TMS are released in the Northern Hemisphere. The equivalent CH₄ emissions values in the Northern Hemisphere for oil, coal, agriculture/waste/landfills, and natural sources are 91%, 88%, 82%, and 54%, respectively. The observed difference between the most Southern (90°S–72°S) and Northern (72°N–90°N) latitudinal band is 134 ppb (7.6% of the global average CH₄ mixing ratio) compared to 177 ppb (10.1%) in the simulation (medium FER scenario) averaged over 1990–2010, which is qualitatively consistent with previous studies.^{35,64} This small North–south (N–S) gradient mismatch between observations and simulation suggests that the simulated CH₄ estimates for each source category could be plausible.

The interhemispheric gradient indicates that total emissions in the medium FER scenario (best global fit in 2000; see Figure 2a) are too high in the North and too low in the South (relative to the simulated a priori data set). Also, the simulated interhemispheric gradient is significantly higher than the observation in all FER scenarios. Because (i) reducing FER alone is not sufficient to match the observed interhemispheric gradient, and (ii) coal and oil CH₄ totals are considered a low estimate (i.e., Northern emissions could be even higher), misallocation of non-FF CH₄ emissions across hemispheres must at least partially explain the N–S mismatch. This is consistent with previous atmospheric inversions, which tend to reduce high latitudinal sources compensated by increases at lower latitudes.^{35,64} Tropical wetlands may be underestimated in particular.³⁵ Further evidence is provided in the SI (section 3.2), which illustrates that NG (or other FFs) are unlikely causes of the N–S mismatch between simulations and observations. Instead, seasonal observations suggest that

wetlands (a reduction in the North and an increase in the South) and/or agriculture/waste/landfills (an increase in the North) were biased in the a priori estimates.

Influence of FER on Life Cycle GHG Emissions of Power Generation Compared with Coal. The life cycle GHG emissions from power generation are frequently estimated to assess the feasibility of replacing coal with NG to mitigate climate change.^{10,11,67–69} Note, however, that other comparisons, for example, use as a transportation fuel,⁷⁰ are also policy-relevant. Corresponding to previous work,^{10,11,67–69} this study estimates the climate implications of NG in terms of CO₂-equivalent (CO₂e) emissions per unit of generated electricity. This metric accounts for the differences in cumulative radiative forcing of CH₄ relative to CO₂ over a given period—commonly 100 and 20 years—using global warming potentials (GWP).⁷¹ Figure 3 compares total life cycle

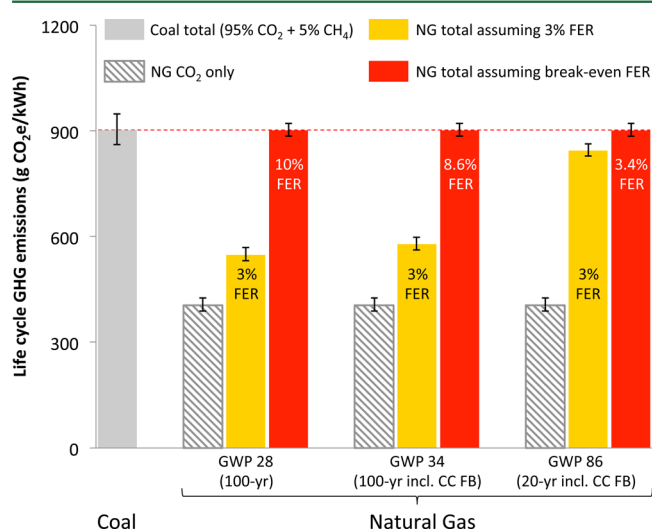


Figure 3. Comparison of life cycle GHG emissions of power generation from coal and NG assuming 39% and 50% conversion efficiency, respectively. Literature estimates for coal^{1,2,11} and NG^{1,2,10,72} CO₂ were used. Yellow and red columns assume 3% FER (mean value of most likely FER range since 2000 from this study) and break-even FER (required to match coal emissions), respectively, using 48 g CO₂e/kWh per percentage point FER from.⁶⁸ NG is shown for three different global warming potentials (GWP; see text). Coal is shown for GWP 28 only because CH₄ contributes only 5% to total emissions. NG error bars include CO₂ only. Coal error bars pertain to combined uncertainty in CO₂ and CH₄ emissions. CC FB: climate-carbon feedbacks (see text).

GHG emissions of power generation from coal and NG assuming 39% and 50% efficiency, respectively. Given a GWP of 28 (100 yr period), and assuming 3% FER (i.e., the mean value of the most likely FER range since 2000 from this study), total NG emissions are about 39% lower than coal. After including climate-carbon feedbacks (CC FB), which account for the impact of the GHGs on other gaseous and aerosol forcing species,⁷¹ this value decreases to 36% (GWP 34). The FER would need to be 10% (excluding CC FB; 8.5% FER including CC FB) in order to reach the same total emissions as coal (break-even point). However, over a 20 yr period, NG already breaks even with coal at 3.4% FER, thus well within the most likely FER range in this study. Results for GWP 84 (20 yr, no CC FB) are not shown in Figure 3 because differences are negligibly small (3.5% break-even FER). Note that this coal-NG comparison excludes potential direct climate effects from

non-GHG climate forcers, such as sulfate aerosols from coal combustion, which may have a cooling effect.²

DISCUSSION

The objective of this top-down study was to estimate global average FER related to the NG life cycle in order to better understand whether recently reported high FER of 6–9%^{1,4} are representative of the larger NG industry. Using a global box-model and well-known quantities of global average atmospheric CH₄, δ¹³C–CH₄, and C₂H₆ mixing ratios, the most likely FER was found to be 2–4% since 2000, and currently (2006–2011) having an upper bound FER of 5%. Both results are potentially overestimated because these estimates exclude highly uncertain emissions from natural hydrocarbon seepage. Taking into account increasing NG (and other FF) production, the FER (in % of dry production) has been declining steadily over time.

The box-model results (most likely FER of 2–4% since 2000) are consistent with those from 3D modeling. The low magnitude of the difference in the interhemispheric gradient between simulations and measurements (less than 5% of the global budget) indicates a minor bias in the simulated emissions sources. The interhemispheric gradient and seasonal comparisons show that an improved spatial emissions allocation includes (i) an emissions transfer from Northern to Southern wetland emissions and/or (ii) increased Northern agriculture/waste/landfills emissions in combination with FER lower than 2–4%. Thus, neither the interhemispheric gradient nor the seasonal comparisons suggest that a global average FER of 2–4% over the period 2000–2011 is too low. This conclusion is subject to potential imprecision of the TMS emissions transport model, which may lead to uncertainties in the simulated spatial allocation of CH₄ emissions. However, this is unlikely given the independent C₂H₆ based box-model upper bound FER of 5%.

The study results lead to both research recommendations and policy implications. A more formal uncertainty analysis of key parameters (atmospheric lifetimes, natural emissions, and NG composition) would provide a more detailed characterization of FER uncertainties. This requires composition data by well type (NG, oil) that are not currently available at this level of detail. Policies aimed at providing such data, for example, publishing international well sample data collected from the oil and gas industry in a central database, would improve the accuracy of FER estimates.

The most likely global FER range (2–4%) is slightly higher than many recent bottom-up estimates (1.1–3.2%; full life cycle) in the U.S. and elsewhere;^{10,51,68,73} however, potentially unaccounted natural seepage could reduce our estimate. Our most recent (2011) global upper bound of 4.4% FER suggests that two recent high estimates of 6–9% in the U.S.^{1,4} may be possible at individual sites, but do not appear representative of the national average unless U.S. NG industry practices are significantly worse than in the rest of the world. When used for power generation, combined NG CH₄ and CO₂ emissions break even with coal at 8.6% FER using a 100-year CH₄ GWP (including CC FB), but the break-even is only 3.4% over 20 years (Figure 3). Thus, despite our relatively low FER estimates, policies to further reduce fugitive emissions appear justified. Shale gas production was too small globally (increasing from 1.5% of global production in 2007 to 5.9% in 2011⁶¹) to yield a signal *even if* FER from shale gas is higher than from conventional NG. However, few bottom-up studies indicate significantly higher FER from shale compared to

conventional gas.⁶⁸ Local and regional top-down studies using field measurements can complement global modeling. These may provide more basin specific FER estimates unattainable with the current global observational network. The NG industry average FER estimates from this work can be used as a reference, and basin specific studies may point to areas with local or regional hot spots.

■ ASSOCIATED CONTENT

● Supporting Information

Literature review of simulated non-FF emissions, observational data description, additional box-model and 3D-model results, and comparison of GHG emissions impacts from NG and coal power generation using global warming potentials. This material is available free of charge via the Internet at <http://pubs.acs.org>.

■ AUTHOR INFORMATION

Corresponding Author

*Phone: (303) 497-5073; fax: (303) 497-5590; e-mail: stefan.schwietzke@noaa.gov.

Present Address

[†]NOAA Earth Systems Research Laboratory, 325 Broadway GMD1, Boulder, CO 80305, United States

Author Contributions

S.S. was responsible for study design, development of box-model and emissions inventory, analysis of 3D-model results, and manuscript preparation. W.M.G. and H.S.M. helped with study design, model analysis, and improved the manuscript. L.B. did 3D-modeling, helped with model analysis, and improved the manuscript. All authors have given approval to the final version of the manuscript.

Notes

The authors declare no competing financial interest.

■ ACKNOWLEDGMENTS

We thank Ed J. Dlugokencky and John B. Miller for valuable comments and discussions. The long-term ethane data are from the UC Irvine global monitoring network (<http://cdiac.ornl.gov/trends/otheratg/blake/blake.html>). This research was made possible through support from the Climate and Energy Decision Making (CEDM) center. This Center has been created through a cooperative agreement between the National Science Foundation (SES-0949710) and Carnegie Mellon University. The ERM Foundation-North America Sustainability Fellowship has provided additional funding.

■ ABBREVIATIONS

CH₄ methane
C₂H₆ ethane
EF emissions factor
FER fugitive emissions rate (% of dry production of NG)
FF fossil fuels (natural gas, oil, coal)
GWP global warming potential
NG natural gas

■ REFERENCES

(1) Howarth, R. W.; Santoro, R.; Ingraffea, A. Methane and the greenhouse-gas footprint of natural gas from shale formations. *Clim. Change* **2011**, *106*, 679–690.
(2) Wigley, T. M. L. Coal to gas: The influence of methane leakage. *Clim. Change* **2011**, *108*, 601–608.

(3) Pétron, G.; et al. Hydrocarbon emissions characterization in the Colorado Front Range: A pilot study. *J. Geophys. Res.* **2012**, *117*, D04304.

(4) Karion, A.; et al. Methane emissions estimate from airborne measurements over a western United States natural gas field. *Geophys. Res. Lett.* **2013**, *40*, 4393–4397.

(5) Miller, S. M.; et al. Anthropogenic emissions of methane in the United States. *Proc. Natl. Acad. Sci. U. S. A.* **2013**, *110*, 20018–20022.

(6) Brandt, A. R.; et al. Methane Leaks from North American Natural Gas Systems. *Science* **2014**, *343*, 733–735.

(7) EPA. Oil and Natural Gas Sector: Reconsideration of Certain Provisions of New Source Performance Standards, Final Rule, 40 CFR Part 60. (2013). <http://www.gpo.gov/fdsys/pkg/FR-2013-09-23/pdf/2013-22010.pdf>.

(8) Allen, D. T.; et al. Measurements of methane emissions at natural gas production sites in the United States. *Proc. Natl. Acad. Sci. U. S. A.* **2013**, *110*, 17768–17773.

(9) API/ANGA. Characterizing Pivotal Sources of Methane Emissions from Natural Gas Production: Summary and Analysis of API and ANGA Survey Responses, 2012.

(10) Venkatesh, A.; Jaramillo, P.; Griffin, W. M.; Matthews, H. S. Uncertainty in life cycle greenhouse gas emissions from united states natural gas end-uses and its effects on policy. *Environ. Sci. Technol.* **2011**, *45*, 8182–8189.

(11) Jiang, M.; et al. Life cycle greenhouse gas emissions of Marcellus shale gas. *Environ. Res. Lett.* **2011**, *6*, 034014.

(12) Gage, B. D.; Driskill, D. L. Analyses of Natural Gases 1917–2007, 2008

(13) Simpson, I. J.; et al. Long-term decline of global atmospheric ethane concentrations and implications for methane. *Nature* **2012**, *488*, 490–494.

(14) Aydin, M.; et al. Recent decreases in fossil-fuel emissions of ethane and methane derived from firm air. *Nature* **2011**, *476*, 198–201.

(15) Levin, I.; et al. No inter-hemispheric $\delta^{13}\text{CH}_4$ trend observed. *Nature* **2012**, *486*, E3–E4.

(16) Miller, J. B. The carbon isotopic composition of atmospheric methane and its constraint on the global methane budget. In *Stable Isotopes and Biosphere Atmosphere Interactions*; Flanagan, L. B., Ehleringer, J. R., Pataki, D. E.; Elsevier, 2005; 288–310.

(17) Kirschke, S.; et al. Three decades of global methane sources and sinks. *Nat. Geosci.* **2013**, *6*, 813–823.

(18) Schwietzke, S.; Griffin, W. M.; Matthews, H. S. Global bottom-up fossil fuel fugitive methane and ethane emissions inventory for atmospheric modeling. *ACS Sustainable Chem. Eng.* **2014**, (<http://dx.doi.org/10.1021/sc500163h>).

(19) ESRL. CarbonTracker-CH₄ documentation. (2013). http://www.esrl.noaa.gov/gmd/ccgg/carbontracker-ch4/documentation_obs.html#ct_doc.

(20) Prinn, R. G.; Huang, J.; Weiss, R. F.; Cunnold, D. M. Evidence for variability of atmospheric hydroxyl radicals over the past quarter century. *Geophys. Res. Lett.* **2005**, *32*, 2–5.

(21) Prather, M. J.; Holmes, C. D.; Hsu, J. Reactive greenhouse gas scenarios: Systematic exploration of uncertainties and the role of atmospheric chemistry. *Geophys. Res. Lett.* **2012**, *39*.

(22) Naik, V.; et al. Preindustrial to present-day changes in tropospheric hydroxyl radical and methane lifetime from the Atmospheric Chemistry and Climate Model Intercomparison Project (ACCMIP). *Atmos. Chem. Phys.* **2013**, *13*, 5277–5298.

(23) Voulgarakis, A.; et al. Analysis of present day and future OH and methane lifetime in the ACCMIP simulations. *Atmos. Chem. Phys.* **2013**, *13*, 2563–2587.

(24) Rudolph, J. The tropospheric distribution and budget of ethane. *J. Geophys. Res. Atmos.* **1995**, *100*, 11369–11381.

(25) Hartmann, D. L. et al. Observations: Atmosphere and surface. In *Climate Change 2013: The Physical Science Basis. Contribution of Working Group I to the Fifth Assessment Report of the Intergovernmental Panel on Climate Change*; Stocker, T. F. et al., Eds.; Cambridge University Press, 2014.

- (26) Krol, M.; et al. The two-way nested global chemistry-transport zoom model TMS: Algorithm and applications. *Atmos. Chem. Phys.* **2005**, *5*, 417–432.
- (27) Bruhwiler, L.; et al. CarbonTracker-CH₄: An assimilation system for estimating emissions of atmospheric methane. *Atmos. Chem. Phys.* **2013**, Submitted.
- (28) Fung, I.; Prather, M.; John, J.; Lerner, J.; Matthews, E. Three-dimensional model synthesis of the global methane cycle. *J. Geophys. Res.* **1991**, *96*, 13033–13065.
- (29) Lassey, K. R.; Lowe, D. C.; Manning, M. R. The Trend in Atmospheric Methane Delta C-13 Implications for Isotopic Constraints on the Global Methane Budget. *Global Biogeochem. Cycles* **2000**, *14*, 41–49.
- (30) Sriskantharajah, S. et al. *Tellus B*; Vol 64 (2012). <http://www.tellusb.net/index.php/tellusb/article/view/18818>.
- (31) Schoell, M. Genetic characterization of natural gases. *Am. Assoc. Pet. Geol. Bull.* **1983**, *67*, 2225–2238.
- (32) Michel, S. E. Institute of Arctic and Alpine Research (INSTAAR), University of Colorado, Boulder. Personal communication. 2014.
- (33) Miller, J. B.; et al. Development of analytical methods and measurements of ¹³C/¹²C in atmospheric CH₄ from the NOAA Climate Monitoring and Diagnostics Laboratory Global Air Sampling Network. *J. Geophys. Res. Atmos.* **2002**, *107*, ACH 11–1–ACH 11–15.
- (34) EIA. *International Energy Statistics*. (2013). <http://www.eia.gov/cfapps/ipdbproject/iedindex3.cfm?tid=2&pid=38&aid=12&cid=regions&syid=1980&eyid=2011&unit=BKWH>.
- (35) Mikaloff Fletcher, S. E.; Tans, P. P.; Bruhwiler, L. M.; Miller, J. B.; Heimann, M. CH₄ sources estimated from atmospheric observations of CH₄ and its ¹³C/¹²C isotopic ratios: 1. Inverse modeling of source processes. *Global Biogeochem. Cycles* **2004**, *18*, GB4004.
- (36) Bousquet, P.; et al. Contribution of anthropogenic and natural sources to atmospheric methane variability. *Nature* **2006**, *443*, 439–443.
- (37) Chen, Y.-H.; Prinn, R. G. Estimation of atmospheric methane emissions between 1996 and 2001 using a three-dimensional global chemical transport model. *J. Geophys. Res. Atmos.* **2006**, *111*.
- (38) Wang, J. S. et al. A 3-D model analysis of the slowdown and interannual variability in the methane growth rate from 1988 to 1997. *Global Biogeochem. Cycles* **2004**, *18*.
- (39) IPCC. *Climate Change 2001: The Physical Science Basis. Contribution of Working Group I to the Third Assessment Report of the Intergovernmental Panel on Climate Change. Chapter 6*, 2001.
- (40) Wuebbles, D. J.; Hayhoe, K. Atmospheric methane and global change. *Earth-Science Rev.* **2002**, *57*, 177–210.
- (41) Ridgwell, A. J.; Marshall, S. J.; Gregson, K. Consumption of atmospheric methane by soils: A process-based model. *Global Biogeochem. Cycles* **1999**, *13*, 59.
- (42) Bergamaschi, P.; et al. Satellite cartography of atmospheric methane from SCIAMACHY on board ENVISAT: 2. Evaluation based on inverse model simulations. *J. Geophys. Res.* **2007**, *112*, 1–26.
- (43) Janssens-Maenhout, G. *EDGAR-HTAP: A Harmonized Gridded Air Pollution Emission Dataset Based on National Inventories*, 2012.
- (44) Matthews, E.; Fung, I.; Lerner, J. Methane emission from rice cultivation: Geographic and seasonal distribution of cultivated areas and emissions. *Global Biogeochem. Cycles* **1991**, *5*, 3.
- (45) Giglio, L.; Van Der Werf, G. R.; Randerson, J. T.; Collatz, G. J.; Kasibhatla, P. Global estimation of burned area using MODIS active fire observations. *Atmos. Chem. Phys.* **2006**, *6*, 957–974.
- (46) Van Der Werf, G. R.; et al. Interannual variability of global biomass burning emissions from 1997 to 2004. *Atmos. Chem. Phys. Discuss.* **2006**, *6*, 3175–3226.
- (47) GFED. Global Fire Emissions Database. (2013). <http://www.globalfiredata.org/>.
- (48) Elvidge, C. D.; et al. A fifteen year record of global natural gas flaring derived from satellite data. *Energies* **2009**, *2*, 595–622.
- (49) Elvidge, C. D.; Baugh, K. E.; Ziskin, D.; Anderson, S.; Ghosh, T. *Estimation of Gas Flaring Volumes Using NASA MODIS Fire Detection Products* 2011.
- (50) IPCC. *2006 IPCC Guidelines for National Greenhouse Gas Inventories, Prepared by the National Greenhouse Gas Inventories Programme. Agric. For. Other L. Use 4*, IGES, 2006.
- (51) EPA. *Inventory of U.S. Greenhouse Gas Emissions and Sinks: 1990–2011*. (2013). <http://www.epa.gov/climatechange/ghgemissions/usinventoryreport.html>.
- (52) Wilson, D.; Fanjoym, J.; Billings, R. *Gulfwide Emission Inventory Study for the Regional Haze and Ozone Modeling Effort*, 2004.
- (53) Wilson, D. *Year 2008 Gulfwide Emission Inventory Study*, 2010.
- (54) EPA. *Reducing Methane Emissions From Coal Mines in China: The Potential for Coalbed Methane Development*, 1996.
- (55) CIRI. *China Coal Industry Yearbook 2009*, 2011.
- (56) EPA. *State Inventory and Projection Tool*. (2012). <http://www.epa.gov/statelocalclimate/resources/tool.html>.
- (57) Fung, I.; Matthews, E. & Lerner, J. Atmospheric methane response to biogenic sources—Results from a 3-D atmospheric tracer model. *Abstr. Pap. Am. Chem. Soc.* **193**, 6–GEOC, 1987.
- (58) Kaplan, J. O. Wetlands at the last glacial maximum: Distribution and methane emissions. *Geophys. Res. Lett.* **2002**, *29*, 3–6.
- (59) Etiope, G.; Ciccioli, P. Earth's degassing: A missing ethane and propane source. *Science* **2009**, *323*, 478.
- (60) Nisbet, E. G.; Dlugokencky, E. J.; Bousquet, P. Methane on the rise—again. *Science* **2014**, *343*, 493–495.
- (61) EIA. U.S. Energy Information Administration. (2014). www.eia.gov.
- (62) Montzka, S. A.; et al. Small interannual variability of global atmospheric hydroxyl. *Science* **2011**, *331*, 67–69.
- (63) Dlugokencky, E. J.; Nisbet, E. G.; Fisher, R.; Lowry, D. Global atmospheric methane: Budget, changes and dangers. *Philos. Trans. R. Soc., A* **2011**, *369*, 2058–2072.
- (64) Houweling, S.; Kaminski, T.; Dentener, F.; Lelieveld, J.; Heimann, M. Inverse modeling of methane sources and sinks using the adjoint of a global transport model. *J. Geophys. Res.* **1999**, *104*, 26137–26160.
- (65) Dlugokencky, E. J.; Steele, L. P.; Lang, P. M.; Masarie, K. A. Atmospheric methane at Mauna Loa and Barrow observatories: Presentation and analysis of in situ measurements. *J. Geophys. Res.* **1995**, *100*, 23103.
- (66) Masarie, K. A.; Tans, P. P. Extension and integration of atmospheric carbon dioxide data into a globally consistent measurement record. *J. Geophys. Res.* **1995**, *100*, 11593.
- (67) NETL. *Life Cycle Greenhouse Gas Inventory of Natural Gas Extraction, Delivery and Electricity Production*, 2011.
- (68) Weber, C. L.; Clavin, C. Life cycle carbon footprint of shale gas: Review of evidence and implications. *Environ. Sci. Technol.* **2012**, *46*, 5688–5695.
- (69) Burnham, A.; et al. Life-cycle greenhouse gas emissions of shale gas, natural gas, coal, and petroleum. *Environ. Sci. Technol.* **2012**, *46*, 619–627.
- (70) Alvarez, R. A.; Pacala, S. W.; Winebrake, J. J.; Chameides, W. L.; Hamburg, S. P. Greater focus needed on methane leakage from natural gas infrastructure. *Proc. Natl. Acad. Sci. U. S. A.* **2012**, *109*, 6435–40.
- (71) Myhre, G. et al. Anthropogenic and natural radiative forcing. In *Climate Change 2013—The Physical Science Basis. The Working Group I Contribution to the Fifth Assessment Report of the Intergovernmental Panel on Climate Change*; Stocker, T. F. et al., Eds.; Cambridge University Press, 2014.
- (72) Jaramillo, P.; Griffin, W. M.; Matthews, H. S. Comparative life-cycle air emissions of coal, domestic natural gas, LNG, and SNG for electricity generation. *Environ. Sci. Technol.* **2007**, *41*, 6290–6296.
- (73) Dienst, C.. *Treibhausgasemissionen des russischen Exportpipeline System – Ergebnisse und Hochrechnungen empirischer Untersuchungen in Russland*, 2004.